Dalton Transactions

COMMUNICATION

View Article Online
View Journal | View Issue

Cite this: *Dalton Trans.*, 2015, **44**, 464

Received 7th July 2014,
Accepted 31st October 2014

DOI: 10.1039/c4dt02056a

www.rsc.org/dalton

A cyano-bridged tubular coordination polymer with dominant ferromagnetic interactions†

Peng-Fei Zhuang, Tao Liu,* Xian-Hui Xie, Cheng He and Chun-Ying Duan

It is a challenge to synthesize a porous tubular coordination polymer with magnetic properties. Utilizing $[Fe^{II}(bipy)(CN)_4]^{2-}$ (bipy = 2,2′-bipyridine) as the building block to react with Mn^{2+}, we successfully synthesized a cyano-bridged tubular coordination polymer with dominant ferromagnetic interactions. The inner surface of the heterometallic tube is hydrophilic, whereas the outer surface is hydrophobic. The framework is stable up to 320 °C and can adsorb N_2 and CO_2. The ferromagnetic interactions were transmitted *via* the diamagnetic N–C–Fe^{II}–C–N species between Mn^{2+} ions in the tube.

The study of coordination polymers has attracted considerable attention due to their fascinating structures and potential applications in various fields.[1] It is known that metal–organic coordination polymers comprise both metal ions and organic ligands, providing the possibility of fabricating multifunctional materials in which more than two different physical properties coexist or interact synergistically.[2] The structures and properties of metal–organic coordination polymers can be modified by choosing functional metal atoms and ligands, which can be synthesized by rational designs based on molecular engineering.[3] An inert and rigid building block is a good candidate to provide directional assembly with controllable structures and physical properties. Hence, metallocyanates have been the subject of extensive research because metallocyanate building blocks are inert and stable molecules that can act as ligands for metal complexes.[4] The linear bridging mode of the cyano group allows a stepwise approach for preparing complexes with predictable architectures. Moreover, the nature of the exchange interaction *via* the cyanide bridge enables chemists to reasonably predict the spin of the ground state and the magnitude of the magnetic anisotropy in some cases.[5] However, it is still a challenge to synthesize a cyano-bridged tubular coordination polymer with magnetic properties. To solve this problem, we proposed using $[Fe^{II}(bipy)(CN)_4]^{2-}$ as a building block to directional assembly with paramagnetic Mn^{2+} ions, providing the magnetic properties for the synthesis of a tubular coordination polymer. Here, a novel cyano-bridged tubular compound $\{[Fe^{II}(bipy)(CN)_4]Mn^{II}(H_2O)\}\cdot H_2O$ (**1**) was synthesized, wherein the ferromagnetic interactions dominate in the framework. Moreover, **1** shows high thermal stability and can adsorb N_2 and CO_2.

1 was synthesized by the reaction of $K_2[Fe^{II}(bipy)(CN)_4]\cdot 3H_2O$ and $Mn(ClO_4)_2\cdot 6H_2O$ in water. Crystallization required several weeks. Single-crystal X-ray diffraction analyses at 296 K revealed that **1** was crystallized in the trigonal space group $R\bar{3}$, presenting an infinite tubular structure with a 1D hexagonal channel along the *c* direction (Fig. S1†). The structure is made up of neutral $\{[Fe^{II}(bipy)(CN)_4]Mn^{II}(H_2O)\}\cdot H_2O$ and non-coordinated solvate water molecules. In **1**, one Fe^{II} (Fe1) and one Mn^{II} (Mn2) are crystallographically independent, and their coordination environments are shown in Fig. 1. The

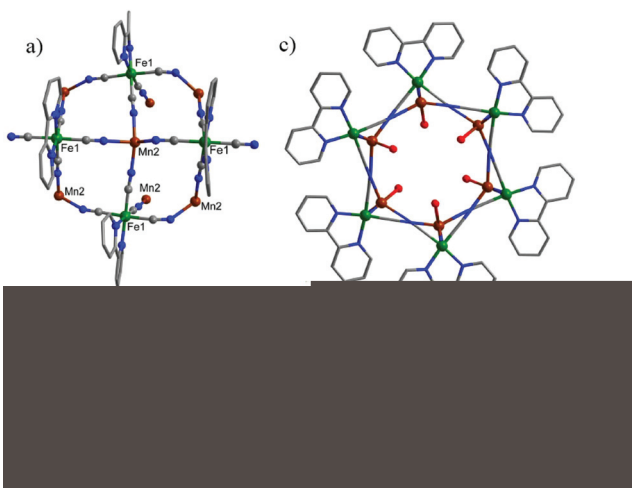

Fig. 1 (a) Coordination environment of Fe and Mn centers in **1**. (b) The hexanuclear Fe_3Mn_3 unit in the *ab* plane. (c) Tube diagram of **1** along the *c*-axis. (d) Side view of the tubular structure. H and O atoms have been omitted for clarity (Fe green, Mn brown, C gray N blue).

State Key Laboratory of Fine Chemicals, Dalian University of Technology, Dalian, 116024, China. E-mail: liutao@dlut.edu.cn

†Electronic supplementary information (ESI) available: Experimental details, XRD spectra, X-ray crystallographic file in CIF format for **1**, Tables S1, Fig. S1–S2 CCDC 994569 (**1**). For ESI and crystallographic data in CIF or other electronic format see DOI: 10.1039/c4dt02056a

Fe1 center is coordinated by four cyanide carbon atoms and two nitrogen atoms of bidentate 2,2 -bipyridine, forming a distorted FeC_4N_2 octahedral coordination environment. Selected bond lengths and angles are presented in Table S1.† The Fe–C bond lengths are 1.886(4)–1.929(4) Å and the Fe–N distances are 1.985(3)–1.995(3) Å, respectively, which is in good agreement with those observed for the low-spin Fe^{II} in an octahedral coordination environment.[6] The Fe–C≡N linkages are almost linear with bond angles of 171.5(3)–177.9(3)°, whereas the Mn2 center is located in a distorted square pyramidal environment with four cyanide nitrogen atoms and an oxygen atom from coordinated water molecules. The Mn–N and Mn–O bond lengths are 2.115(4)–2.166(3) Å and 2.363(3) Å, respectively, which is similar to those observed in the related complexes.[4d] The axial Mn–N≡C bond angles deviate distinctly from linearity with bond angles of 140.4(3)° and 159.0(3)°. The equatorial Mn–N≡C bond angles are closer to linearity with bond angles of 175.4(3)° and 175.7(3)°. As shown in Fig. 1a, each $[Fe^{II}(bipy)(CN)_4]^{2-}$ unit acts as a tetradentate bridging ligand to four manganese(II) ions through its four cyanide groups in the equatorial/axial(2 : 2) positions, while each manganese(II) ion is connected to four $[Fe^{II}(CN)_4(bipy)]^{2-}$ units. The N≡C–Fe–C≡N plane related to the axial cyano groups is almost perpendicular to the Mn–N≡C–Fe plane related to the equatorial cyano groups by a dihedral angle of 89.7°. The equatorial Fe–Mn distances are 5.158(2) and 5.168(2) Å, and the axial Fe–Mn distances are 4.860(2) and 5.130(2) Å. As shown in Fig. 1b, in the *ab* plane, three Fe^{II} ions and three Mn^{II} ions are alternately bridged by six cyano groups, forming a hexanuclear Fe_3Mn_3 unit. Interestingly, three Fe^{II} ions and three Mn^{II} ions construct a regular triangle with an edge of 9.821(2) Å and 7.403(2) Å, respectively. Within the tube, the hydrogen bonding interactions were formed between the coordinated water molecules with the donor acceptor distance O1···O1·of 2.760(6) Å. In addition, six metal ions of the Fe_3Mn_3 units are nearly *coplanar* with a mean deviation of 0.34 Å. Moreover, along the *c*-axis, the Fe^{II} and Mn^{II} ions are alternately bridged by axial cyano groups. In this manner, all the hexanuclear Fe_3Mn_3 units are assembled alternately to form an infinite 1D tubular structure with a hexagonal channel. After removing all water molecules, the tube has an internal 1D channel with a diameter of 2.4 Å, excluding the van der Waals radii of the surface atoms (Fig. 1c). The tube comprises six identical sides, and each side runs along the *c* direction in a distorted ladder-like structure (Fig. 1d). Each coordination tube is surrounded by six neighboring identical coordination tubes with a distance of 16.82(2) Å between the centers of the two closest tubes (Fig. S1†). The non-coordinated water molecules reside in the tubular cavity, and the potential void volume, calculated by PLATON, was 11.8% when the water molecules were removed.

The temperature-dependent magnetic susceptibilities (χ) of **1** were measured in the temperature range of 2–300 K under a 1000 Oe field (Fig. 2a). At 300 K, the χT value was 4.43 $cm^3 mol^{-1}$ K per FeMn unit. As the temperature decreased, the χT values gradually increased to a maximum value of 9.14 $cm^3 mol^{-1}$ K at 2 K. This behavior indicates that the ferromagnetic

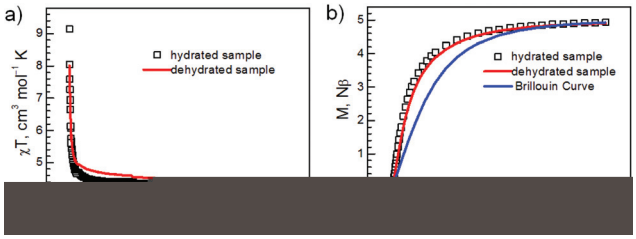

Fig. 2 (a) Temperature-dependent magnetic susceptibilities of **1** and the dehydrated sample in the temperature range of 2–300 K under an applied field of 1000 Oe. (b) Field dependence of magnetization for **1** and the dehydrated sample at 1.8 K. The blue solid line is the calculated Brillouin curve of the isolated Mn^{2+} ion.

interaction dominates in this system. In the temperature range of 2–300 K, the magnetic susceptibility data are fitted to the Curie–Weiss law with a Curie constant C of 4.4 $cm^3 mol^{-1}$ K and a Weiss constant θ of 0.34 K. This C value is in agreement with a magnetically isolated manganese(II) ion. The positive Weiss temperature further confirms the dominant ferromagnetic interaction in this temperature region. Moreover, the ferromagnetic coupling is also supported by the field dependence of magnetization for **1** at 1.8 K,[7] as shown in Fig. 2b. As the applied magnetic field increases, the isothermal magnetization increases almost linearly at low fields and reaches a saturation value of 5.0$N\beta$ at 50 kOe, which corresponds to the predicted saturation value (5.0$N\beta$ for one Mn^{II}, assuming g = 2.00) for an S = 5/2 magnetically isolated high-spin manganese(II) ion. The magnetization of **1** is significantly higher than the Brillouin curve corresponding to non-interacting S_{Mn} spins (S = 5/2), confirming ferromagnetic interactions in **1** (Fig. 2b). It has been reported that the N–C–Fe^{II}–C–N species can transmit ferromagnetic interactions between Fe^{III} (S = 5/2) ions although the magnetic exchange through diamagnetic anions is weak.[8] Moreover, the hydrogen bonding can transmit ferromagnetic interactions.[9] We measured the magnetic properties of the dehydrated sample to determine whether the ferromagnetic interactions were transmitted *via* the diamagnetic N–C–Fe^{II}–C–N species or hydrogen bonding. It was found that the magnetic properties of **1** and the dehydrated sample were very similar. Because there is no hydrogen bonding in the dehydrated sample, the ferromagnetic interactions should be transmitted *via* the diamagnetic N–C–Fe^{II}–C–N species between Mn^{II} ions in **1** and the dehydrated sample.

Thermal gravimetric analysis (TGA) of the crystalline sample powder of **1** was performed in the temperature range of 25–800 °C under a N_2 atmosphere (Fig. S2†). The initial mass loss of 9.3% in the temperature range of 25 °C to approximately 110 °C in the TGA data corresponds to the loss of all coordinated water molecules and solvent water molecules (calculated as 8.9%), which is consistent with the single crystal data. A plateau is observed from 110 to 320 °C, indicating that **1** has high thermal stability until 320 °C. Above 320 °C, **1** shows a rapid weight loss due to the decomposition of the framework. The powder X-ray diffraction patterns of **1** and dehydrated **1** are almost identical (Fig. S3†), indicating

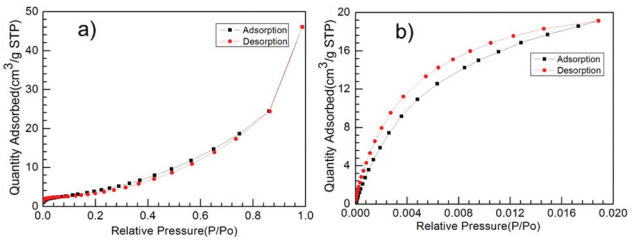

Fig. 3 (a) Adsorption/desorption isotherms of N_2 at 77 K. (b) Adsorption/desorption isotherms of CO_2 for dehydrated **1** at 273 K.

that the framework is stable after removal of the water molecules, implying that dehydrated **1** has excellent thermal stability. This stability has provided an opportunity for probing the gas adsorption properties of dehydrated **1**.

The gas adsorption properties of dehydrated **1** for N_2 at 77 K and CO_2 at 273 K were evaluated (Fig. 3). The maximum uptake of N_2 for dehydrated **1** is 46.03 $cm^3\ g^{-1}$ at 77 K and 1 atm, with a reversible type I behavior, confirming the microporous nature of dehydrated **1**.[10] The Brunauer–Emmett–Teller (BET) surface area of dehydrated **1**, calculated from the maximum value of the N_2 adsorption isotherm, is estimated to be 10.49 $m^2\ g^{-1}$ with a pore volume of 0.069 $cm^3\ g^{-1}$. This small pore volume is reasonable because dehydrated **1** has only a 1D channel along the *c*-axis.[11] Interestingly, the CO_2 sorption isotherms for dehydrated **1** also exhibited typical type I isotherms with a steep initial increase at low pressures and saturation at higher pressures, and with a slight hysteresis on desorption.[12] The type I isotherms observed with abrupt adsorption at very low pressures are common for microporous materials. The presence of hysteresis may contribute to the existence of intercrystalline voids or the diffusion of CO_2 inside the pores appears to experience some restrictions.[13] There is no significant CO_2 uptake for dehydrated **1**, and the adsorption amount is only 19.13 mL g^{-1} at 273 K. These are comparable to the uptake capacities of some highly porous zeolitic imidazolate frameworks, which are in the range of 19–55 mL g^{-1} under the same conditions.[14]

Conclusions

In summary, we have successfully constructed a novel tubular coordination polymer with dominant ferromagnetic interactions in the tube using metallocyanate as a building block. The inner surface of the tube is hydrophilic, whereas the outer surface is hydrophobic. The magnetic tubular coordination polymer exhibits permanent porosity for gas sorption of CO_2 and N_2, providing a strategy to synthesize multi-functional materials.

Acknowledgements

This work was partly supported by the NSFC (grants 21421005, 91122031, and 21322103) and the Fundamental Research Funds for the Central Universities, China.

Notes and references

1 (*a*) C. Benelli and D. Gatteschi, *Chem. Rev.*, 2002, **102**, 2369; (*b*) C. Edder, C. Piguet, J. C. G. Bunzli and G. Hopfgartner, *Chem. – Eur. J.*, 2001, **7**, 3014; (*c*) H. J. Choi and M. P. Suh, *J. Am. Chem. Soc.*, 2004, **126**, 15844; (*d*) C. D. Wu, A. Hu and W. B. Lin, *J. Am. Chem. Soc.*, 2005, **127**, 8940; (*e*) B. Kesanli, Y. Cui, M. R. Smith, E. W. Bittner, B. L. Bockrath and W. Lin, *Angew. Chem., Int. Ed.*, 2005, **44**, 72.

2 (*a*) W. Eerenstein, N. D. Mathur and J. F. Scott, *Nature.*, 2006, **442**, 759; (*b*) M. K. Singh, Y. Yang and C. G. Takoudis, *Coord. Chem. Rev.*, 2009, **253**, 2920; (*c*) L. Hou, W. X. Zhang, J. P. Zhang, W. Xue, Y. B. Zhang and X.-M. Chen, *Chem. Commun.*, 2010, **46**, 6311; (*d*) D. K. Unruh, K. Gojdas, A. Libo and T. Z. Forbes, *J. Am. Chem. Soc.*, 2013, **135**, 7398.

3 F. Chang, Z. M. Wang, H. L. Sun, S. Gao, G. H. Wen and X. X. Zhang, *Dalton Trans.*, 2005, 2976.

4 (*a*) M. Verdaguer, A. Bleuzen, V. Marvaud, J. Vaissermann, M. Seuleiman, C. Desplanches, A. Scuiller, C. Train, R. Garde, G. Gelly, C. Lomenech, I. Rosenman, P. Veillet, C. Cartier and F. Villain, *Coord. Chem. Rev.*, 1999, **190–192**, 1023; (*b*) M. Ohba and H. Ōkawa, *Coord. Chem. Rev.*, 2000, **198**, 313; (*c*) J. Černák, M. Orendáč, I. Potočňák, J. Chomič, A. Orendáčová, J. Skoršepa and A. Feher, *Coord. Chem. Rev.*, 2002, **224**, 51; (*d*) J. Xia, W. Shi, X. Y. Chen, H. S. Wang, P. Cheng, D. Z. Liao and S. P. Yan, *Dalton Trans.*, 2007, 2373; (*e*) S. Nastase, C. Maxim, M. Andruh, J. Cano, C. Ruiz-Perez, J. Faus, F. Lloret and M. Julve, *Dalton Trans.*, 2011, **40**, 4898; (*f*) R. Lescouëzec, L. M. Toma, J. Vaissermann, M. Verdaguer, F. S. Delgado, C. RuizPérez, F. Lloret and M. Julve, *Coord. Chem. Rev.*, 2005, **249**, 2691; (*g*) Y. Z. Zhang, S. Gao, Z. M. Wang, G. Su, H. L. Sun and F. Pan, *Inorg. Chem.*, 2005, **44**, 4534.

5 (*a*) T. Liu, H. Zheng, S. Kang, Y. Shiota, S. Hayami, M. Mito, O. Sato, K. Yoshizawa, S. Kanegawa and C. Duan, *Nat. Commun.*, 2013, **4**, 2826; (*b*) O. Kahn and C. J. Martinez, *Science*, 1998, **279**, 44; (*c*) D. F. Li, S. Parkin, G. B. Wang, G. T. Yee, A. V. Prosvirin and S. M. Holmes, *Inorg. Chem.*, 2005, **44**, 4903; (*d*) W. X. Zhang, R. Ishikawa, B. Breedlove and M. Yamashita, *RSC Adv.*, 2013, **3**, 3772; (*e*) K. Mitsumoto, M. Ui, M. Nihei, H. Nishikawa and H. Oshio, *Crystengcomm*, 2010, **12**, 2697; (*f*) A. Mondal, Y. Li, P. Herson, M. Seuleiman, M. L. Boillot, E. Riviere, M. Julve, L. Rechignat, A. Bousseksou and R. Lescouezec, *Chem. Commun.*, 2012, **48**, 5653; (*g*) J. F. Letard, J. A. Real, N. Moliner, A. B. Gaspar, L. Capes, O. Cador and O. Kahn, *J. Am. Chem. Soc.*, 1999, **121**, 10630; (*h*) M. Nihei, M. Ui, M. Yokota, L. Q. Han, A. Maeda, H. Kishida, H. Okamoto and H. Oshio, *Angew. Chem., Int. Ed.*, 2005, **44**, 6484.

6 (*a*) J. Mercurol, Y. Li, E. Pardo, O. Risset, M. Seuleiman, H. Rousseliere, R. Lescouezec and M. Julve, *Chem. Commun.*, 2010, **46**, 8995; (*b*) T. Liu, Y. J. Zhang, S. Kanegawa and O. Sato, *Angew. Chem., Int. Ed.*, 2010, **49**, 8645; (*c*) M. Nihei, Y. Sekine, N. Suganami, K. Nakazawa, A. Nakao, H. Nakao, Y. Murakami and H. Oshio, *J. Am. Chem. Soc.*, 2011, **133**, 3592.

7 (*a*) L. M. Toma, C. Ruiz-Perez, F. Lloret and M. Julve, *Inorg. Chem.*, 2012, **51**, 1216; (*b*) S. Wang, J. L. Zuo, H. C. Zhou, Y. Song, S. Gao and X. Z. You, *Eur. J. Inorg. Chem.*, 2004, 3681.

8 (*a*) I. Salitros, R. Boca, R. Herchel, J. Moncol, I. Nemec, M. Ruben and F. Renz, *Inorg. Chem.*, 2012, **51**, 12755; (*b*) I. Nemec, T. Šilha, R. Herchel and Z. Trávníček, *Eur. J. Inorg. Chem.*, 2013, 5781.

9 (*a*) K. Wang, Y. Q. Wang, X. M. Zhang and E. Q. Gao, *Dalton Trans.*, 2013, **42**, 4533; (*b*) W. Plass, A. Pohlmann and J. Rautengarten, *Angew. Chem., Int. Ed.*, 2001, **40**, 4207.

10 (*a*) J. Liang and G. K. H. Shimizu, *Inorg. Chem.*, 2007, **46**, 10449; (*b*) H. Li, Z. Niu, T. Han, Z. Zhang, W. Shi and P. Cheng, *Sci. China: Chem.*, 2011, **54**, 1423.

11 R. A. Agarwal, A. Aijaz, C. Sañudo, Q. Xu and P. K. Bharadwaj, *Cryst. Growth Des.*, 2013, **13**, 1238.

12 (*a*) J. J. Jiang, M. Pan, J. M. Liu, W. Wang and C. Y. Su, *Inorg. Chem.*, 2010, **49**, 10166; (*b*) P. Pachfule, R. Das, P. Poddar and R. Banerjee, *Cryst. Growth Des.*, 2011, **11**, 1215; (*c*) X. Zhou, Z. Zhang, B. Li, F. Yang, Y. Peng, G. Li, Z. Shi, S. Feng and J. Li, *New J. Chem.*, 2013, **37**, 425; (*d*) P. Wang, L. Luo, J. Fan, G. C. Lv, Y. Song and W. Y. Sun, *Microporous Mesoporous Mater.*, 2013, **175**, 116.

13 (*a*) J. Seo, N. Jin and H. Chun, *Inorg. Chem.*, 2010, **49**, 10833; (*b*) B. Zheng, J. Luo, F. Wang, Y. Peng, G. Li, Q. Huo and Y. Liu, *Cryst. Growth Des.*, 2013, **13**, 1033.

14 A. Phan, C. J. Doonan, F. J. Uribe-Romo, C. B. Knobler, M. O'Keeffe and O. M. Yaghi, *Acc. Chem. Res.*, 2009, **43**, 58.